Remodeling of the Plasma Membrane by Surface-Bound Protein Monomers and Oligomers: The Critical Role of Intrinsically Disordered Regions

Mussie K. Araya[1], **Yong Zhou**[1], **Alemayehu A. Gorfe**[1]

[1]Department of Integrative Biology and Pharmacology, McGovern Medical School, University of Texas Health Science Center at Houston, 6431 Fannin St., Houston, TX 77030, USA

Abstract

The plasma membrane (PM) of cells is a dynamic structure whose morphology and composition is in constant flux. PM morphologic changes are particularly relevant for the assembly and disassembly of signaling platforms involving surface-bound signaling proteins, as well as for many other mechanochemical processes that occur at the PM surface. Surface-bound membrane proteins (SBMP) require efficient association with the PM for their function, which is often achieved by the coordinated interactions of intrinsically disordered regions (IDRs) and globular domains with membrane lipids. This review focuses on the role of IDR-containing SBMPs in remodeling the composition and curvature of the PM. The ability of IDR-bearing SBMPs to remodel the Gaussian and mean curvature energies of the PM is intimately linked to their ability to sort subsets of phospholipids into nanoclusters. We therefore discuss how IDRs of many SBMPs encode lipid-binding specificity or facilitate cluster formation, both of which increase their membrane remodeling capacity, and how SBMP oligomers alter membrane shape by monolayer surface area expansion and molecular crowding.
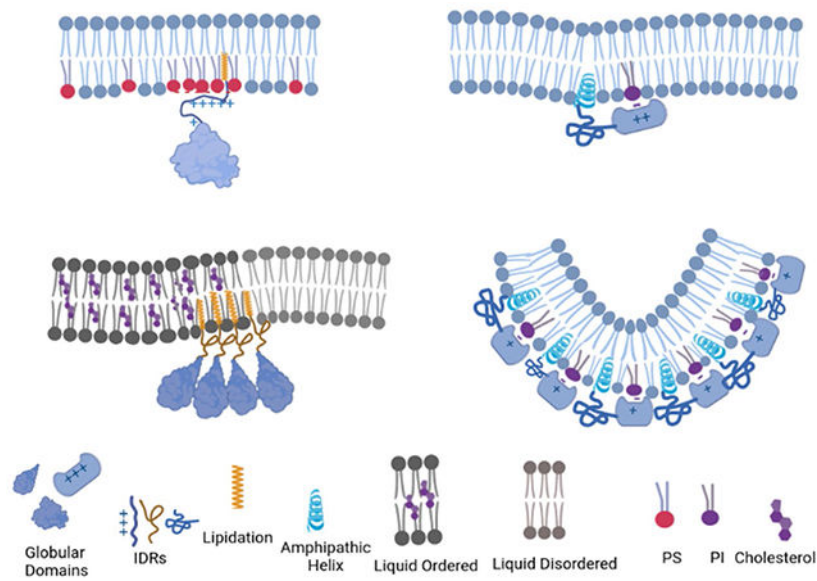
Graphical Abstract

✉Alemayehu A. Gorfe, Alemayehu.G.Abebe@uth.tmc.edu.

Competing interests The authors declare no competing interests.

Conflict of interest The authors declare no conflict of interest.

Globular Domains | IDRs | Lipidation | Amphipathic Helix | Liquid Ordered | Liquid Disordered | PS | PI | Cholesterol

Keywords

Introduction

The Lipid Bilayer and Membrane Mechanics

Biological membranes are soft assemblies of lipids, proteins and carbohydrates (Singer and Nicolson 1972). Cells devote ~ 5% of their genes to synthesize 200–1000 lipid species (van Meer et al. 2008). Phospholipids account for more than 50% of the total lipid content of the plasma membrane (PM). The most prevalent phospholipids include phosphatidylcholine (PC), phosphatidylserine (PS), phosphatidylethanolamine (PE), phosphatidic acid (PA), and phosphoinositide (PI) (van Meer et al. 2008; Suetsugu et al. 2014). Sphingolipids such as sphingomyelin (SM) constitute another class of phospholipids found in the PM. PC and SM are mostly found in the outer leaflet of the PM while PE, PS and PI are more common in the inner leaflet (Park et al. 2021). The PM also contains sterols such as cholesterol, which accounts for ~ 20% by weight of eukaryotic cell membranes (Naito et al. 2019). The amphiphilic nature of phospholipids allows them to spontaneously self-assemble into a bilayer in an aqueous solvent (Lodish and Rothman 1979). PC, PS and SM have a cylindrical geometry and thus organize into a planar bilayer. In contrast, PE and cholesterol do not form bilayer on their own, and PE imposes a negative curvature stress on bilayers due to its conical geometry (Raja 2011; Suetsugu et al. 2014). Thus, membrane curvature is in part determined by the packing geometry of the constituent lipids (Israelachvili et al. 1976). One way to achieve membrane remodeling, such as during the formation of membrane domains, is therefore via the selective synthesis of specific lipid species. A good example for this is provided by synaptic vesicles, which contain high levels of curvature-causing cholesterol (40 mol%) and PE (20%) relative to PC (17%), PS (6%) or SM (3.6%) (Binotti

et al. 2021). The highly curved presynaptic PM is also enriched with lipids possessing poly-unsaturated chains whose coneshaped geometry favors curvature (Breckenridge et al. 1972; Baumgart et al. 2005; Marszalek and Lodish 2005; Takamori et al. 2006).

Biological membranes including the PM are thin (~ 4 nm) compartments with a large surface area (e.g., the surface of a typical spherical cell with a diameter of 20–1200 μm^2) (Pfenninger 2009). As a result, membranes favor bending over in-plane stresses. Micropipette aspiration experiments using giant membrane vesicles showed that the bending stuffiness of phosphatidylcholine bilayers is in the range of 14–30 K_BT, depending on the chain length of the lipids (Rawicz et al. 2000). Similar experiments on PC vesicles containing 0 and 10 mol% cholesterol found that bending stiffness is dependent on cholesterol content (Meleard et al. 1997), with the stiffness increasing with cholesterol content in bilayers made up of saturated PC lipids and decreasing with cholesterol content in sphingomyelin bilayers (Garcia et al. 2010). While bending stiffness > 50 K_BT has been measured in some sphingomyelin/cholesterol giant vesicles (Garcia et al. 2010), the comparatively low stiffness (10–20 K_BT) in bilayers of physiologic lipid composition allows molecular collisions and nanoscale energy released by catabolic reactions to induce bending of membranes (Servuss et al. 1976; Schneider et al. 1984; Lifshitz et al. 1986; Strey et al. 1995; Do Carmo 2016). This renders the PM sensitive to manipulation by membrane proteins including surface-bound (or peripheral) membrane proteins (SMBPs).

Theories have been developed to describe the energetics of membrane remodeling underpinned by changes in bending stiffness due to alterations in lipid composition or the action of membrane proteins. Briefly, according to the classical Helfrich theory of membrane bending, the free energy of bending per unit area can be described by Gaussian and ordinary curvatures (Helfrich 1973) (Box 1; Eq. 1). Gaussian curvature is critical for membrane topological transformations that occur, for example, during membrane fission and viral budding. The cost of deforming a membrane during viral budding and vesicle recycling thus includes Gaussian energy, E_G, that can be described by the saddle splay modulus $\bar{\kappa}$ or the integral of the Gaussian curvature K over the membrane surface (**S**), as defined in Eq. 4 below and Box 1,

$$E_G = \bar{\kappa} \int_S K \cdot d\mathbf{S} = 2\pi X \bar{\kappa},$$

(4)

where X is the Euler characteristic of the surface (Box 1). This expression is applicable to cases of membrane topological transformations without concomitant changes in membrane phase behavior. When there is phase separation or domain formation (of different $\bar{\kappa}$), the Gauss–Bonnet theorem (Eq. 2 in Box 1) gives rise to an additional term involving a line integral along the domain boundary that accounts for the line tension between domains (Eq. 5). We substitute the surface integral of Gaussian curvature in Eq. 4 by the term given in the Gauss–Bonnet theorem in Eq. 2 of Box 1 and obtain:

$$E_G = \bar{\kappa} \int_S K \cdot d\mathbf{S} = 2\pi \bar{\kappa} X - \bar{\kappa} \oint_C k_g \cdot d\mathbf{l} \,.$$

(5)

A change in Gaussian curvature energy is therefore associated with changes in line tension along domain boundaries (Lipowsky 1992; Jülicher and Lipowsky 1993), and/or changes in topology of the membrane surface. Similarly, discontinuity of the saddle splay modulus at the interface of domain boundaries triggers an instability for a non-zero neck radius of a budding vesicle and its ultimate fission (Allain et al. 2004).

Topological transformations are typically preceded (e.g., budding) and succeeded (e.g., sealing following fission) by smaller scale membrane deformations involving ordinary (non-Gaussian) bending energy in the order of $\sim 8\pi\kappa$ ($>> K_B T$). An example is the intermediate stalk formation, a transition state between a planar membrane and a vesicle that results from spontaneous monolayer curvature (Kozlovsky and Kozlov 2002). This curvature can generate a substantial constriction force at the membrane neck that depends on the mean curvature J and the spontaneous curvature c_0 (Igli and Rappolt 2019; Lipowsky et al. 2020; Steinkühler et al. 2020; Lipowsky 2022) (Eq. 6):

$$f = 8\pi\kappa(J - c_o).$$

(6)

Surface–Bound Membrane Proteins

Proteins represent an important constituent of the PM and account for approximately 50% of its mass (Duncan et al. 2017). These include transmembrane proteins that sit across the PM and surface-bound membrane proteins (SBMPs) that reside on one side of the PM. The latter include proteins harboring unstructured polycationic regions that interact with anionic membrane lipids (e.g., the KRAS protein that specifically interacts with PS) (Takenawa and Itoh 2006; Lemmon 2008), structural folds with a binding pocket for specific phospholipids (e.g., Pleckstrin homology domains that recognize PIs) (Cozier et al. 2004), and scaffolds that bind membranes non-specifically (e.g., BAR domains). Many SBMPs contain intrinsically disordered regions (IDRs) that serve either as the primary site of membrane engagement or complement other membrane targeting motifs. IDRs are segments that lack a well-defined tertiary structure (Dyson and Wright 2005), and may include partially or fully unstructured random coils and flexible linkers. The structural plasticity of IDRs endows them with binding promiscuity, enhanced sensitivity to environmental cues, and ease of activity modulation by post-translational modifications (Oldfield and Dunker 2014; Granata et al. 2015). IDRs play key roles in mediating membrane association of SBMPs. An important class of SBMPs that use IDRs as their primary means of membrane binding are post-translationally lipid-modified proteins involved in a wide variety of cell signaling processes (Gorfe and Hocker 2012). These proteins mostly reside at the cytosolic side of membranes, such as the inner leaflet of the PM (Gorfe and Hocker 2012). This is achieved by inserting the covalently lipidated IDR into one leaflet of the membrane (Ferguson 1991; Casey and Seabra 1996; Novelli and D'Apice 2011). The most common lipid modifications in mammalian cells include myristoylation, which is the addition of a 14-carbon saturated fatty acid chain to an N-terminal glycine; palmitoylation, the addition of a 16-carbon saturated palmitoyl chain to a cysteine side chain; and prenylation, the addition of a 15- (farnesyl) or 20- (geranylgeranyl) carbon poly-unsaturated and branched fatty acid to C-terminal cysteine residues (Resh 2006; Wilson et al. 2011). IDRs are also

common in non-lipidated SBMPs, playing key roles in membrane binding and lipid sorting. The interactions of IDRs with lipids and their role in regulating cell signaling events have been reviewed recently (Cornish et al. 2020). Similarly, the major classes of membrane proteins involved in membrane curvature generation and/or sensing have been the subject of recent reviews [e.g., (Has and Das 2021; Steinem and Meinecke 2021)]. Expanding the excellent review by Has et al. (2022), here we focus on the remodeling of the PM by structural disorder of SBMPs, including the role of IDRs in lipid sorting, shape changes, and topological transformations. We refer the reader to recent (Has and Das 2021) and earlier reviews (Drin and Antonny 2010; Suetsugu et al. 2014) for the discussion of PM remodeling by globular protein domains.

Membrane Remodeling by Lipidated Surface-Bound Proteins with Intrinsically Disordered Regions

In this section, we discuss membrane remodeling by IDR-containing lipidated SBMPs using the RAS small GTPases, the HIV Gag Matrix protein and, to a lesser extent, the tyrosine-protein kinase Src as illustrative examples. RAS small GTPases must be anchored to the PM for their biological activity (Willumsen et al. 1984; Welman et al. 2000; Jaumot et al. 2002; Abankwa and Gorfe 2020). All RAS isoforms, HRAS, NRAS and splice variants KRAS4A and KRAS4B, which share a highly conserved catalytic G-domain (residues 1–166, > 90% sequence homology) but differ at the hypervariable C terminus residues (167–185/186, < 20% sequence homology), are farnesylated on their C-terminal cysteine residue 185/186 (Hancock et al. 1990; Abankwa et al. 2007; Linder and Deschenes 2007). An additional signal is needed to properly anchor RAS to the PM. In particular, HRAS is dual-palmitoylated on Cysteine 181 and Cysteine 184, NRAS is mono-palmitoylated on Cysteine 181, while KRAS4B (hereafter referred to as KRAS) has a hexa-lysine polybasic domain (residues 175–180) (Zhou et al. 2021a; b). Another example of lipidated SBMP is the retroviral Gag protein, a key orchestrator of PM remodeling during the assembly of the Human Immunodeficiency Virus type 1 (HIV-1) particles (Gelderblom 1991; Bieniasz 2009; Balasubramaniam and Freed 2011). The HIV-1 Gag polyprotein contains three major structural domains, namely the matrix (MA), capsid (CA) and nucleocapsid (NC), as well as two spacer peptides, sp1 and sp2, and an unstructured C terminus p6 peptide. The 132 amino acid N-terminal MA domain, which targets Gag to the PM (Muriaux and Darlix 2010), is characterized by high levels of disorder at its N- and C termini plus a relatively more ordered mid-section. The MA domain also contains an N-terminal myristoyl modification and a polybasic domain that recognizes phosphoinositol 4,5-bisphosphate (PIP_2) in the host PM (Saad et al. 2006). A third example of lipidated membrane-bound proteins is the proto-oncogene tyrosine-protein kinase Src (c-Src), a non-receptor tyrosine kinase protein. This protein contains SH2 and SH3 domains plus a tyrosine kinase domain (Arbesú et al. 2017). Like HIV Gag, c-Src is anchored to the membrane via a combination of a myristoyl moiety and a patch of basic residues (Arbesú et al. 2017).

Lipidated SBMPs and Phase Separation of Membranes

The lipidated IDR of RAS proteins, the HIV Gag protein, and the c-Src kinase contributes to their distinct preferences for cholesterol-enriched liquid-ordered (Lo) or cholesterol-poor liquid-disordered (Ld) domains in the PM (Fig. 1). In particular, electron microscopy

(EM)-spatial analysis quantified the lateral spatial nanoclustering of immunogold-labeled GFP-tagged RAS proteins on intact PM sheets of mammalian cells with or without acute cholesterol depletion via methyl β-cyclodextrin (MβCD) (Prior et al. 2003). The results showed that MβCD treatment effectively disrupted the nanoclustering of inactive GDP-bound HRAS suggesting that inactive HRAS favors Lo domains. Moreover, atomic force microscopy (AFM) and atomically detailed molecular dynamics (MD) simulations have shown that active and inactive KRAS as well as active HRAS prefer Ld domains while activated NRAS prefers Lo domains (Prior et al. 2003; Weise et al. 2011; Janosi et al. 2012; Zhou et al. 2012). EM spatial analysis and MD simulations together further showed that KRAS nanoclusters selectively enrich mixed-chain PS species in Ld domains in synthetic supported bilayers (SBLs), intact PM sheets from cells, and live cell PM (Zhou et al. 2021a; b). Similarly, MD simulations predicted that insertion of the N-terminal myristoyl group of the HIV Gag protein leads to the clustering of 16:0/18:1 phosphatidylserine (POPS) and PIP_2 lipids around the polybasic residues (Monje-Galvan and Voth 2020). In liposomes composed of POPS and POPC, HIV-1 Gag strongly preferred lipids with dual-unsaturated chains over mixed-chain species (Monje-Galvan and Voth 2020). In lipid vesicles and SBLs containing anionic lipids mimicking the PM inner leaflet and the high sterol and SM content of raft domains, the HIV Gag protein induced the assembly of cholesterol-enriched PIP_2 nanoclusters (Yandrapalli et al. 2016; Monje-Galvan and Voth 2020). Thus, the HIV-1 Gag MA domain induces the formation of cholesterol/PIP_2 nanoclusters that include PS with dual-unsaturated chains. AFM experiments also showed that insertion of the myristoyl chain and residues 2–9 of c-Src in anionic (DPPC/DOPC/DPPG/DOPG/Chol 45:20:5:5:25) raft membranes compromised the preexisting Lo/Ld phase separation (Murray et al. 1998).

Backbone conformational fluctuations of the IDR are important for the remodeling of PM lipid composition by our example lipidated SBMPs (Zhou et al. 2017, 2021a; b). Specifically, MD simulations have shown that the farnesylated polybasic domain of KRAS samples 2–3 distinct conformational states upon binding to symmetric PC/PS (Zhou et al. 2017) as well as asymmetric PC-PC/PS and PC-PC/PS/PE bilayers (Araya and Gorfe 2022). The more extended conformations favor PS more (Zhou et al. 2017), particularly mixed-chain PS species (Zhou et al. 2017, 2021a; b). Similarly, the polycationic myristoylated MA domain of HIV Gag displayed distinct backbone conformational preferences and conformation-dependent side chain-lipid interactions (Yandrapalli et al. 2016). In a similar manner, it was found that the conformational dynamics of the N-terminal myristoylated polybasic backbone of the c-Src contributed to its ability to interact with select lipid species (Pons 2021).

Membrane Curvature Sensing by SMBPs

Direct remodeling of lipid composition implies that lipidated surface-bound proteins can modulate mesoscopic membrane properties, because lipid sorting promotes changes in the Gaussian membrane curvature and its associated splay curvature modulus (Box 1). Gaussian curvature contains additional terms for each domain boundary through a line integral over the geodesic curve along the domain boundary (Box 1 and Eq. 5). Along these geodesic curves, there exists a non-zero interfacial tension caused by the hydrophobic mismatch between lipids in different membrane domains, which changes the splay modulus

associated with the Gaussian curvature energy. The effect of boundary line tension on curvature is discussed in many previous reports (Baumgart et al. 2003, 2005; Kuzmin et al. 2005; Zimmerberg and Kozlov 2006), and is proportional to differences between membrane constituent lipids in saturation level and chain order. For example, previous semi-atomistic MD simulations of the HRAS minimal membrane anchor in a DPPC/DLiPC/cholesterol bilayer found that clustering of the anchors at domain boundaries significantly lowers the line tension in the peptide-bound monolayer (Janosi et al. 2012; Li and Gorfe 2013a, b). A systematic analysis of de-palmitoylated and de-farnesylated HRAS membrane anchors and quantification of pressure tensors further showed that line tension and curvature at the phase boundary is highly dependent on the nature of the lipid modification (Janosi et al. 2012; Li and Gorfe 2013a, b). The sorting of lipids with specific head groups or acyl chains into nanodomains in the PM of living cells will likely remodel the Gaussian curvature in even more complex ways than found in the ternary (DPPC/DilPC/Cholesterol) model bilayers used in the simulations (Fig. 2).

Related to the remodeling of Gaussian curvature by surface-bound RAS proteins is their ability to sense changes in curvature. The local geometry on a 2D surface in 3D space can be defined by the two principal curvatures, or the mean and Gaussian curvature (Box 1). For example, spherical vesicles and cylindrical tubes have distinct Gaussian curvatures, and varying their diameter leads to changes in the mean curvature. Larsen et al. examined the ability of the NRAS membrane anchor to sense changes in Gaussian curvature. Specifically, the spatial segregation of the NRAS membrane anchor was found to depend on the Gaussian curvature of spherical vesicles and tubes of varying diameters (Larsen et al. 2020). The partitioning of proteins into membrane domains involves the interplay between protein-lipid interactions and steric effects, the former being mainly determined by the chemical properties of the protein components and the latter dominated by lipid packing and protein volume (Lin et al. 2018). A molecular field analysis suggested that the response of the NRAS membrane anchor to changes in Gaussian curvature is primarily determined by lateral pressure (Larsen et al. 2015, 2020). Changes in lateral pressure may underlie Gaussian curvature sensing by SBMPs more broadly (Janosi et al. 2012; Li and Gorfe 2013a, b; Larsen et al. 2020), consistent with concomitant changes in lateral pressure and line tension observed during simulations of the HRAS lipid-anchor clustering at membrane domain boundaries (Li and Gorfe 2013a, b). Sensing of membrane curvature may also depend on the conformational entropy and net charge of IDPs/IDRs. For example, through a quantitative analysis of fluorescently labeled small unilamellar vesicles, Zeno et al. showed that electrostatics dominates the curvature sensing ability of SBMPs with highly charged and short IDRs, while entropic effects dominate in longer IDRs with fewer charged residues (Zeno et al. 2019).

RAS proteins may also alter bilayer shape in smaller scales. This local bilayer structure perturbation depends on the insertion depth and localization of the IDR's backbone and side chains, as shown for HRAS (Gorfe et al. 2007a; b) and KRAS (Janosi and Gorfe 2010) using MD simulations. While the HRAS membrane anchor with its two palmitoyl chains tends to insert deeper into bilayers and thereby increase thickness in its vicinity (Gorfe et al. 2004, 2007a, 2008, 2007b), the KRAS membrane anchor has a shallower insertion depth and thins the bilayer in its vicinity (Janosi and Gorfe 2010). This is consistent with another study

showing that HRAS and KRAS membrane anchors possess distinct membrane curvature preferences in cells (Liang et al. 2019). Specifically, an increase in positive PM curvature resulted in elevated nanoclustering and PM localization of HRAS while disrupting those of KRAS (Liang et al. 2019).

Similarly, membrane remodeling by the HIV Gag MA protein during viral assembly involves substantial changes in the Gaussian (She et al. 2018; Dharmavaram et al. 2019; Sengupta and Lippincott-Schwartz 2020) and ordinary bending energies. Sorting of lipids by this protein into nanodomains results in changes in bending stiffness and spontaneous curvature, generating a substantial constriction force at the viral budding site (see Eq. 6) (Lipowsky 2022). Cholesterol/PIP$_2$/PS-enriched HIV Gag MA nanodomains are separated from the surrounding membrane by domain boundaries, with the associated line tension adding to the Gaussian curvature stress (Lipowsky 1992; Jülicher and Lipowsky 1993; Jülicher and Lipowsky 1996; Kozlovsky and Kozlov 2003; Baumgart et al. 2005; Lipowsky 2022) (Box 1; Eq. 5). Domain boundaries may also reduce structural and topological transition barriers and thereby facilitate budding (Baumgart et al. 2003; Riske et al. 2006; Dreher et al. 2021). Indeed, the Gaussian curvature modulus $\bar{\kappa}$ (Eq. 7) and its monolayer counterpart $\bar{\kappa}_m$ (Eq. 8) can be expressed as the second moment of a membrane's lateral stress profile $\sigma(z)$, taken over the bilayer or, when centered at the pivotal plane z_0, a monolayer (Helfrich 1981a, b; Hamm and Kozlov 2000). Currently, it is not feasible to measure the stress profile in experiments, but it is readily accessible in simulations although not without challenges (Hu et al. 2012, 2013; Venable et al. 2015).

$$\bar{\kappa} = \int_{-\frac{h}{2}}^{\frac{h}{2}} \sigma(z)z^2 dz, \tag{7}$$

$$\bar{\kappa}_m = \int_0^{\frac{h}{2}} \sigma(z - z_0)z^2 dz. \tag{8}$$

Other lipidated proteins such as caveolins combine palmitoylation with membrane-interacting helices to form hairpin-like inclusions that insert into one leaflet of a membrane (Monier et al. 1995). These hairpin-like structures in caveolins and related proteins often form membrane coats and cause curvature via monolayer area expansion and other factors (Simons and Ikonen 1997; Bauer and Pelkmans 2006).

Membrane Remodeling by Non-lipidated Surface-Bound Membrane Proteins

Non-lipidated SBMPs with IDRs are also potent drivers of PM remodeling during, for example, membrane trafficking and recycling. These include protein domains that utilize an amphipathic helix (AH) (Hristova et al. 1999; Seelig 2004), hydrophobic loops, or curved surfaces to bind membranes (Suetsugu et al. 2014). AHs insert their hydrophobic face into the hydrophobic core of the membrane while their polar face localizes at the membrane-water interface (Drin and Antonny 2010). Membrane binding of proteins via an AH may be complemented by lipidation, and the helix may not fold until after membrane

binding. Upon binding, amphipathic helices can induce positive, negative or zero Gaussian curvature to the host membrane (Schmidt and Wong 2013; Tenchov et al. 2013; Simunovic et al. 2016a, b). Cationic residues that typically exist at these helices interact with anionic phospholipids near the site of curvature, thereby contributing to lipid sorting and membrane curvature (Harries et al. 2004). Classic examples of AH-containing membrane binding domains include Bin/Amphiphysin/Rvs (BAR) domains and epsin N-terminal homology (ENTH) domains. Membrane targeting by other structural folds is also often accompanied by the insertion of an AH (Suetsugu et al. 2014; Chen et al. 2016) (see Fig. 3). Similar other wedge-shaped hydrophobic structures (Campelo et al. 2008) that insert into one leaflet of a membrane play many critical roles in trafficking by forming vesicle coats (Bauer and Pelkmans 2006).

Among their many functions, proteins containing BAR and ENTH domains participate in the various stages of clathrin-mediated endocytosis of synaptic vesicles, and cluster PIP_2 lipids at clathrin-coated pits (Bassereau et al. 2018). The N terminus of N-BAR is unfolded in solution but folds into a helix upon inserting into membrane, inducing positive curvature to the membrane (Bhatia et al. 2010; Cui et al. 2011). Curvature is further stabilized by the dimerization of the protein. Endophilin is an example of proteins containing an N-BAR domain, which induces constriction and scission of Ω-shaped clathrin-coated pits during vesicle budding (Perera et al. 2006; Morlot et al. 2012). Endophilin also induces curvature at high density by forming scaffolds that mechanically constrain bud necks and spontaneously tubulate membranes (Shi and Baumgart 2014; Simunovic et al. 2015) (see next section on oligomerization). An example of ENTH-containing SBMPs is epsin. Epsins contain a disordered N-terminal domain that interacts with PIP_2 and folds into an AH, which inserts deep into the hydrophobic core of the membrane like a wedge to induce positive curvature (Masuda et al. 2006). In addition to contacts made by the AH, membrane binding is also stabilized by electrostatic interactions between protein side chains in the rest of the ENTH domain and anionic phospholipids. Other studies of ENTH domains have shown that curvature is generated not only by the insertion of specific domains but also by molecular clustering (Stachowiak et al. 2012a, b; Zeno et al. 2018). Whether the main driving force for membrane remodeling by ENTH is cluster formation (Stachowiak et al. 2012a, 2013, 2012b) or if the two mechanisms (i.e., clustering and insertion) are mutually exclusive remains to be elucidated (Steinem and Meinecke 2021). BAR and ENTH domains also possess hydrophobic regions whose membrane association helps form highly curved deformations and extremely narrow tubules (Suetsugu et al. 2014; Bassereau et al. 2018). Moreover, as alluded to above using caveolins as an example, the asymmetric insertion of AHs, or any other domain for that matter, in one leaflet of a bilayer increases the area of that leaflet relative to the opposing leaflet; the bilayer curves to compensate for the resulting increase in area strain. See Box 2 and Eq. 9 for the energetics of membrane remodeling by monolayer surface area expansion.

Membrane Remodeling by Protein Oligomerization

Membrane remodeling processes are inherently multiscale in both space and time. One way to expand the spatiotemporal scale of membrane deformation is to complement the comparatively small scale deformations induced by individual proteins by larger scale

transformations by protein oligomers. Along this line, experiments on lipid vesicles have shown that both differential area expansion upon the asymmetric insertion of individual SBMPs, as well as lateral steric pressure due to molecular crowding by protein oligomers, play roles in lipid sorting and membrane bending (Zeno et al. 2018, Fakhree et al. 2019a, b) (Fig. 4).

Clustering of SBMPs and Membrane Curvature

Pioneering work by Lipowsky demonstrated that high-density binding of particles on one side of a membrane surface causes the membrane to adopt a curved shape, owing to the difference in steric pressure on the two membrane surfaces (Lipowsky 1995). At the mechanistic level, the greater frequency of collisions among the polymer molecules on the more densely coated surface overcomes the opposing pressure on the less densely coated side, leading to a pressure gradient that relaxes only when the membrane takes on a non-zero curvature (Lipowsky 2007; Bassereau et al. 2018). Depending on the extent of the gradient, the resulting curvature can be quite high. Indeed, concentrated patches of membrane-anchored globular proteins are capable of transforming membrane surfaces into tubules of high curvature (Stachowiak et al. 2010).

It was hypothesized that bulky IDRs occupy considerably larger volumes in comparison with structured motifs of equivalent molecular weight, and IDRs may thus induce larger steric surface pressures and thereby more curvature (Bassereau et al. 2018). Indeed, IDRs are among the most potent drivers of membrane vesiculation and fission (Busch et al. 2015; Snead et al. 2017). Perhaps for the same reason, the IDR-containing RAS proteins form clusters of ~ 6 proteins and average radius of ~9 nm (Plowman et al. 2005), and clustering is important for their ability to sense membrane curvature (Zhou and Hancock 2015; Liang et al. 2019). Note that bilayers tend to bend at the boundaries of co-existing domains in order to minimize the line tension between the domains. Structural, geometrical and stress field analyses of coarse-grained MD trajectories showed that aggregation of HRAS at domain boundaries stabilizes curvature (Janosi et al. 2012; Li and Gorfe 2013a, b; Li and Gorfe 2014). The reduction of the line tension at domain boundaries observed in these simulations can be linked to the remodeling of Gaussian curvature via Eq. 5. Similarly, the observed self-assembly of the HIV-1 Gag protein into higher order oligomers during viral budding (O'Carroll et al. 2013) likely causes substantial changes in Gaussian curvature. Additional examples abound. These include endocytic factors that accomplish the scission of membrane catenoids/saddle by self-assembly and aggregation (Frost et al. 2008; Simunovic et al. 2016). For example, endophilin utilizes its N-BAR domain to drive its own endocytosis (Simunovic et al. 2017), while aggregates of the inverse I-BAR domains induce separation between low- and high-density phases and thereby membrane curvature that eventually leads to scission at the necks (Prévost et al. 2015; Simunovic et al. 2017).

In contrast to many of the reports noted above, it has been suggested that the membrane-inserting motif of endophilin has no potency to induce membrane curvature (Chen et al. 2016), instead emphasizing the role of scaffolding and clustering in membrane remodeling by N-BAR proteins. It has also been shown using optical tweezer experiments on membrane nanotubes that endophilin may directly mediate scission of membrane tubes (Simunovic et

al. 2016). However, this study also showed the requirement of external factors to promote tube elongation, where the significance of molecular clustering may lie. We believe the role of AH in membrane topological transformations cannot be ignored completely, because the extent of membrane fragmentation and reticulation by epsins and N-BARs is correlated with the number of AHs in individual proteins (Boucrot et al. 2012; Simunovic et al. 2013). Therefore, the insertion of AH may likely play a role in the initial destabilization of the membrane (Simunovic et al. 2016) while molecular clustering drives curvature formation associated with vesicle budding and scission. Along this line, experiments on lipid vesicles have suggested that multiple domains of varying Gaussian bending stiffness or saddle splay modulus are requirements for vesicle scission (Allain et al. 2004).

Oligomer Size and Steric Pressure

Recent experiments of IDR-containing endocytic proteins bound to vesicles (diameter = 50 nm) provided insights into the relationship between SBMP oligomer size and capacity to generate steric pressure (Busch et al. 2015; Snead et al. 2017). It was found that the ability of ENTH domains to drive membrane tubulation (Stachowiak et al. 2012a; b) and vesiculation is correlated to the fractional coverage of the membrane surface by the protein (Snead et al. 2017). AP180 and Epsin, which contain IDRs with a large radius of gyration, were shown to be more effective at crowding the membrane surface and driving bending than ENTH domains that have a smaller radius of gyration (Fakhree et al. 2019a; b). Differences in membrane surface area coverage (70 vs 15 μm^2) were correlated with differences in energy from steric pressure (Stachowiak et al. 2012a, b; Bassereau et al.2018). A recent work has shown that Epsin can also induce membrane tubulation using its disordered C terminus via a mechanism by which multiple bulky disordered regions induce curvature through steric pressure (Busch et al. 2015). Similarly, multimers of Epsin combine to drive membrane curvature in simulations. It has been hypothesized that, in response to binding the clathrin adaptor AP2, the radius of the Epsin disordered region expands, further inducing curvature (Kozlovsky and Kozlov 2003). Moreover, BAR scaffolds assemble during membrane fission, and crowding of their bulky disordered domains generates steric pressure that destabilizes lipid tubules (Snead et al. 2019). The increasing appreciation of the role of SBMP/IDR crowding provides for a stochastic view of membrane fission (Snead and Stachowiak 2018), suggesting a shift from a long held paradigm where membrane fission was thought to be driven by proteins with certain tertiary structures.

Conclusion

The PM of cells is a very dynamic structure that constantly undergoes remodeling because of a plethora of phenomena that rely on the generation, modulation, and maintenance of membrane curvature. Many lipidated and non-lipidated surface-bound membrane proteins (SBMPs) containing intrinsically disordered regions (IDRs) undergo conformational changes and clustering upon membrane binding, which result in lipid sorting and membrane remodeling. IDRs that form liquid-like assemblies on membranes are emerging as potent drivers of membrane bending to generate diverse membrane shapes. A better mechanistic understanding of how these IDRs precisely interact with lipids and remodel membranes will shed more light on mechanosensing and mechanotransduction.

This requires new experimental, simulation and modeling studies focused on deciphering the relative roles of mean and Gaussian curvatures in SBMP-induced membrane remodeling.

Acknowledgements

Data Availability

All data used in this review are included in the manuscript.

References

Abankwa D et al. (2007) Ras nanoclusters: molecular structure and assembly. Semin Cell Dev Biol 18(5):599–607 [PubMed: 17897845]

Abankwa D, Gorfe AA (2020) Mechanisms of Ras membrane organization and signaling: Ras rocks again. Biomolecules. 10.3390/biom10111522

Allain JM et al. (2004) Fission of a multiphase membrane tube. Phys Rev Lett 93(15):158104 [PubMed: 15524946]

Araya MK, Gorfe AA (2022) Phosphatidylserine and phosphatidylethanolamine asymmetry have negligible effect on the global structure, dynamics and interactions of the KRAS lipid anchor. J Phys Chem B 126(24):4491–4500 [PubMed: 35687481]

Arbesú M et al. (2017) The unique domain forms a fuzzy intramolecular complex in Src family kinases. Structure 25(4):630–640.e634 [PubMed: 28319009]

Balasubramaniam M, Freed EO (2011) New insights into HIV assembly and trafficking. Physiology 26(4):236–251 [PubMed: 21841072]

Bassereau P et al. (2018) The 2018 biomembrane curvature and remodeling roadmap. J Phys D. 10.1088/1361-6463/aacb98

Bauer M, Pelkmans L (2006) A new paradigm for membrane-organizing and -shaping scaffolds. FEBS Lett 580(23):5559–5564 [PubMed: 16996501]

Baumgart T et al. (2003) Imaging coexisting fluid domains in biomembrane models coupling curvature and line tension. Nature 425(6960):821–824 [PubMed: 14574408]

Baumgart T et al. (2005) Membrane elasticity in giant vesicles with fluid phase coexistence. Biophys J 89(2):1067–1080 [PubMed: 15894634]

Bhatia VK et al. (2010) A unifying mechanism accounts for sensing of membrane curvature by BAR domains, amphipathic helices and membrane-anchored proteins. Semin Cell Dev Biol 21(4):381–390 [PubMed: 20006726]

Bieniasz PD (2009) The cell biology of HIV-1 virion genesis. Cell Host Microbe 5(6):550–558 [PubMed: 19527882]

Binotti B et al. (2021) An overview of the synaptic vesicle lipid composition. Archi Bioch Biophys 709:108966

Boucrot E et al. (2012) Membrane fission is promoted by insertion of amphipathic helices and is restricted by crescent BAR domains. Cell 149(1):124–136 [PubMed: 22464325]

Breckenridge WC et al. (1972) The lipid composition of adult rat brain synaptosomal plasma membranes. Biochim Biophys Acta 266(3):695–707 [PubMed: 4339171]

Busch DJ et al. (2015) Intrinsically disordered proteins drive membrane curvature. Nat Commun 6(1):1–11

Campelo F et al. (2008) The hydrophobic insertion mechanism of membrane curvature generation by proteins. Biophys J 95(5):2325–2339 [PubMed: 18515373]

Casey PJ, Seabra MC (1996) Protein prenyltransferases. J Biol Chem 271(10):5289–5292 [PubMed: 8621375]

Chen Z et al. (2016) The N-terminal amphipathic helix of endophilin does not contribute to its molecular curvature generation capacity. J Amn Chem Soc 138(44):14616–14622

Cornish J et al. (2020) Intrinsically disordered proteins and membranes: a marriage of convenience for cell signalling? Biochem Soc Trans 48(6):2669–2689 [PubMed: 33155649]

Cozier G et al. (2004) Membrane targeting by pleckstrin homology domains. Curr Top Microbiol Immunol 282:49–88 [PubMed: 14594214]

Cui H et al. (2011) Mechanism of membrane curvature sensing by amphipathic helix containing proteins. Biophys J 100(5):1271–1279 [PubMed: 21354400]

Deserno M (2015) Fluid lipid membranes: from differential geometry to curvature stresses. Chem Ohys Lipids 185:11–45

Dharmavaram S et al. (2019) Gaussian curvature and the budding kinetics of enveloped viruses. PLoS Comput Biol 15(8):e1006602 [PubMed: 31433804]

Do Carmo MP (2016) Differential geometry of curves and surfaces: revised and updated, 2nd edn. Courier Dover Publications, Mineola

Dreher Y et al. (2021) Division and regrowth of phase-separated giant unilamellar vesicles. Angew Chem Int Ed 60(19):10661–10669

Drin G, Antonny B (2010) Amphipathic helices and membrane curvature. FEBS Lett 584(9):1840–1847 [PubMed: 19837069]

Duncan AL et al. (2017) Protein crowding and lipid complexity influence the nanoscale dynamic organization of ion channels in cell membranes. Sci Rep 7(1):16647 [PubMed: 29192147]

Dyson HJ, Wright PE (2005) Intrinsically unstructured proteins and their functions. Nat Rev Mol Cell Biol 6:197–208 [PubMed: 15738986]

Fakhree MAA et al. (2019a) Shaping membranes with disordered proteins. Archiv Biochem Biophys 677:108163

Fakhree MAA et al. (2019b) Cooperation of helix insertion and lateral pressure to remodel membranes. Biomacromol 20(3):1217–1223

Ferguson MAJ (1991) Lipid anchors on membrane proteins. Curr Opin Struct Biol 1(4):522–529

Frost A et al. (2008) Structural basis of membrane invagination by F-BAR domains. Cell 132:807–817 [PubMed: 18329367]

Garcia R et al. (2010) Effect of cholesterol on the rigidity of saturated and unsaturated membranes: fluctuation and electrodeformation analysis of giant vesicles. Soft Matt 6(1472–1482):6

Gelderblom HR (1991) Assembly and morphology of HIV: potential effect of structure on viral function. AIDS 5(6):617–637 [PubMed: 1652977]

Gorfe AA et al. (2004) Membrane localization and flexibility of a lipidated ras peptide studied by molecular dynamics simulations. J Am Chem Soc 126(46):15277–15286 [PubMed: 15548025]

Gorfe AA et al. (2007a) H-ras protein in a bilayer: interaction and structure perturbation. J Am Chem Soc 129(40):12280–12286 [PubMed: 17880077]

Gorfe AA et al. (2007b) Structure and dynamics of the full-length lipid-modified H-Ras protein in a 1,2-dimyristoylglycero-3-phosphocholine bilayer. J Med Chem 50(4):674–684 [PubMed: 17263520]

Gorfe AA et al. (2008) Water-membrane partition thermodynamics of an amphiphilic lipopeptide: an enthalpy-driven hydrophobic effect. Biophys J 95(7):3269–3277 [PubMed: 18621822]

Gorfe AA and Hocker HJ (2012) Membrane targeting: methods. In Encyclopedia of Life Sciences(eLS), John Wiley & Sons, Ltd: Chichester. 10.1002/9780470015902.a0002615.pub2

Granata D et al. (2015) The inverted free energy landscape of an intrinsically disordered peptide by simulations and experiments. Sci Rep 5(1):1–15

Hamm M, Kozlov M (2000) Elastic energy of tilt and bending of fluid membranes. Eur Phys J E 3(4):323–335

Hancock JF et al. (1990) A polybasic domain or palmitoylation is required in addition to the CAAX motif to localize p21ras to the plasma membrane. Cell 63(1):133–139 [PubMed: 2208277]

Harries D et al. (2004) Enveloping of charged proteins by lipid bilayers. J Phys Chem B 108(4):1491–1496

Has C et al. (2022) Insights into membrane curvature sensing and membrane remodeling by intrinsically disordered proteins and protein regions. J Membr Biol 255(2–3):237–259 [PubMed: 35451616]

Has C, Das SL (2021) Recent developments in membrane curvature sensing and induction by proteins. Biochim Biophys Acta Gen Subj 1865(10):129971 [PubMed: 34333084]

Helfrich W (1973) Elastic properties of lipid bilayers: theory and possible experiments. Zeitschrift Für Naturforschung C 28(11–12):693–703

Helfrich W (1981a) Amphiphilic mesophases made of defects. Phys Defects 35:716–755

Helfrich W (1981b) Physics of defects. In: Balian R et al. (eds) Les Houches Session XXXV. North-Holland, Amsterdam

Hristova K et al. (1999) An amphipathic α-helix at a membrane interface: a structural study using a novel X-ray diffraction method. J Mol Biol 290(1):99–117 [PubMed: 10388560]

Hu M et al. (2012) Determining the Gaussian curvature modulus of lipid membranes in simulations. Biophys J 102(6):1403–1410 [PubMed: 22455923]

Hu M et al. (2013) Gaussian curvature elasticity determined from global shape transformations and local stress distributions: a comparative study using the MARTINI model. Faraday Discuss 161:365–382 [PubMed: 23805750]

Igli A, Rappolt M (2019) Advances in biomembranes and lipid self-assembly. Academic Press, Cambridge

Israelachvili J et al. (1976) Theory of self-assembly of hydrocarbon amphiphiles into micelles and bilayers. J Chem Soc Faraday Trans 2:72

Janosi L et al. (2012) Organization, dynamics, and segregation of Ras nanoclusters in membrane domains. Proc Natl Acad Sci USA 109(21):8097–8102 [PubMed: 22562795]

Janosi L, Gorfe AA (2010) Segregation of negatively charged phospholipids by the polycationic and farnesylated membrane anchor of Kras. Biophys J 99(11):3666–3674 [PubMed: 21112291]

Jaumot M et al. (2002) The linker domain of the Ha-Ras hypervariable region regulates interactions with exchange factors, Raf-1 and phosphoinositide 3-kinase. J Biol Chem 277(1):272–278 [PubMed: 11689566]

Jülicher F, Lipowsky R (1993) Domain-induced budding of vesicles. Phys Rev Lett 70(19):2964 [PubMed: 10053698]

Jülicher F, Lipowsky R (1996) Shape transformations of vesicles with intramembrane domains. Phys Rev E 53(3):2670

Kozlovsky Y, Kozlov MM (2002) Stalk model of membrane fusion:solution of energy crisis. Biophys J 82(2):882–895 [PubMed: 11806930]

Kozlovsky Y, Kozlov MM (2003) Membrane fission: model for intermediate structures. Biophys J 85(1):85–96 [PubMed: 12829467]

Kuzmin PI et al. (2005) Line tension and interaction energies of membrane rafts calculated from lipid splay and tilt. Biophys J 88(2):1120–1133 [PubMed: 15542550]

Larsen JB et al. (2015) Membrane curvature enables N-Ras lipid anchor sorting to liquid-ordered membrane phases. Nat Chem Biol 11(3):192–194 [PubMed: 25622090]

Larsen JB et al. (2020) How membrane geometry regulates protein sorting independently of mean curvature. ACS Cent Sci 6(7):1159–1168 [PubMed: 32724850]

Lee JM (1997) The Gauss-Bonnet theorem. In: Lee JM (ed) Riemannian manifolds: an introduction to curvature. Springer, New York, pp 155–172

Lemmon MA (2008) Membrane recognition by phospholipid-binding domains. Nat Rev Mol Cell Biol 9(2):99–111 [PubMed: 18216767]

Li Z, Gorfe AA (2013a) Deformation of a two-domain lipid bilayer due to asymmetric insertion of lipid-modified Ras peptides. Soft Matt. 10.1039/C3SM51388B

Li Z, Gorfe AA (2013b) Aggregation of lipid-anchored full-length H-Ras in lipid bilayers: simulations with the MARTINI force field. PLOS One 10.1371/journal.pone.0071018

Li H, Gorfe AA (2014) Membrane remodeling by surface-bound protein aggregates: insights from coarse-grained molecular dynamics simulation. J Phys Chem Lett 5(8):1457–1462 [PubMed: 24803997]

Liang H et al. (2019) Membrane curvature sensing of the lipid-anchored K-Ras small GTPase. Life Sci Alliance. 10.26508/lsa.201900343

Lifshitz EM, Kosevich AM, Pitaevskii LP (1986) Chapter II—the equilibrium of rods and plates. In: Lifshitz EM, Kosevich AM, Pitaevskii LP (eds) Theory of elasticity, 3rd edn. Butterworth-Heinemann, Oxford, pp 38–86

Lin X et al. (2018) Protein partitioning into ordered membrane domains: insights from simulations. Biophys J 114(8):1936–1944 [PubMed: 29694870]

Linder ME, Deschenes RJ (2007) Palmitoylation: policing protein stability and traffic. Nat Rev Mol Cell Biol 8(1):74–84 [PubMed: 17183362]

Lipowsky R (1992) Budding of membranes induced by intramembrane domains. J Physique II 2(10):1825–1840

Lipowsky R (1995) Bending of membranes by anchored polymers. EPL (europhysics Letters) 30(4):197

Lipowsky R (2007) Bending of membranes by anchored polymers. EPL (europhysics Letters) 30:197

Lipowsky R et al. (2020) The giant vesicle book. Milton & Park, Taylor Francis

Lipowsky R (2022) Remodeling of membrane shape and topology by curvature elasticity and membrane tension. Adv Biol (weinh) 6(1):e2101020 [PubMed: 34859961]

Lodish HF, Rothman JE (1979) The assembly of cell membranes. Scie Am 240(1):48–63

Marszalek JR, Lodish HF (2005) Docosahexanoid acid, fatty-acid interacting proteins, and neuronal function: breastmilk and fish are good for you. Annu Rev Cell Dev Biol 21(1):633–657 [PubMed: 16212510]

Masuda M et al. (2006) Endophilin BAR domain drives membrane curvature by two newly identified structure-based mechanisms. EMBO J 25(12):2889–2897 [PubMed: 16763557]

Mazharimousavi SH et al. (2017) Generalized monge gauge. Int J Geom Methods Mod 14(04):1750062

Meleard P et al. (1997) Bending elasticities of model membranes: influences of temperature and sterol content. Biophys J 72(6):2616–2629 [PubMed: 9168037]

Monier S et al. (1995) VIP21-caveolin, a membrane protein constituent of the caveolar coat, oligomerizes in vivo and in vitro. Mol Biol Cell 6(7):911–927 [PubMed: 7579702]

Monje-Galvan V, Voth GA (2020) Binding mechanism of the matrix domain of HIV-1 gag on lipid membranes. Elife. 10.7554/eLife.58621

Morlot S et al. (2012) Membrane shape at the edge of the dynamin helix sets location and duration of the fission reaction. Cell 151(3):619–629 [PubMed: 23101629]

Muriaux D, Darlix J-L (2010) Properties and functions of the nucleocapsid protein in virus assembly. RNA Biol 7(6):744–753 [PubMed: 21157181]

Murray D et al. (1998) Electrostatics and the membrane association of Src: theory and experiment. Biochemistry 37(8):2145–2159 [PubMed: 9485361]

Naito T et al. (2019) Movement of accessible plasma membrane cholesterol by the GRAMD1 lipid transfer protein complex. Elife 8:e51401 [PubMed: 31724953]

Novelli G, D'Apice MR (2011) Protein farnesylation and disease. J Inherit Metab Dis 35:917–926

O'Carroll IP et al. (2013) Elements in HIV-1 Gag contributing to virus particle assembly. Virus Res 171(2):341–345 [PubMed: 23099087]

Oldfield CJ, Dunker AK (2014) Intrinsically disordered proteins and intrinsically disordered protein regions. Annu Rev Biochem 83:553–584 [PubMed: 24606139]

Park S et al. (2021) Developing initial conditions for simulations of asymmetric membranes: a practical recommendation. Biophys J 120(22):5041–5059 [PubMed: 34653389]

Perera RM et al. (2006) Two synaptojanin 1 isoforms are recruited to clathrin-coated pits at different stages. Proc Natl Acad Sci USA 103(51):19332–19337 [PubMed: 17158794]

Pfenninger KH (2009) Plasma membrane expansion: a neuron's Herculean task. Nat Rev Neurosci 10(4):251–261 [PubMed: 19259102]

Plowman SJ et al. (2005) H-ras, K-ras, and inner plasma membrane raft proteins operate in nanoclusters with differential dependence on the actin cytoskeleton. Proc Natl Acad Sci USA 102(43):15500–15505 [PubMed: 16223883]

Pons M (2021) Basic residue clusters in intrinsically disordered regions of peripheral membrane proteins: modulating 2D diffusion on cell membranes. Physchem 1(2):152–162

Prévost C et al. (2015) IRSp53 senses negative membrane curvature and phase separates along membrane tubules. Nat Commun 6(1):8529 [PubMed: 26469246]

Prior IA et al. (2003) Direct visualization of Ras proteins in spatially distinct cell surface microdomains. J Cell Biol 160(2):165–170 [PubMed: 12527752]

Raja M (2011) Do small headgroups of phosphatidylethanolamine and phosphatidic acid lead to a similar folding pattern of the K(+) channel? J Membr Biol 242(3):137–143 [PubMed: 21744243]

Rawicz W et al. (2000) Effect of chain length and unsaturation on elasticity of lipid bilayers. Biophys J 79(1):328–339 [PubMed: 10866959]

Resh MD (2006) Trafficking and signaling by fatty-acylated and prenylated proteins. Nature Chem Biol 2:584–590 [PubMed: 17051234]

Riske KA et al. (2006) Electrofusion of model lipid membranes viewed with high temporal resolution. Biophys Rev Lett 1(04):387–400

Saad JS et al. (2006) Structural basis for targeting HIV-1 Gag proteins to the plasma membrane for virus assembly. Proc Natl Acad Sci USA 103(30):11364–11369 [PubMed: 16840558]

Schmidt NW, Wong GC (2013) Antimicrobial peptides and induced membrane curvature: geometry, coordination chemistry, and molecular engineering. Curr Opin Solid State Mater Sci 17(4):151–163 [PubMed: 24778573]

Schneider MB et al. (1984) Thermal fluctuations of large cylindrical phospholipid vesicles. Biophys J 45(5):891–899 [PubMed: 6733240]

Seelig J (2004) Thermodynamics of lipid–peptide interactions. Biochim Biophys Acta 1666(1–2):40–50 [PubMed: 15519307]

Sengupta P, Lippincott-Schwartz J (2020) Revisiting membrane microdomains and phase separation: a viral perspective. Viruses. 10.3390/v12070745

She B, Dharmavaram S, Rouzina I, Bruinsma R (2018) Role of Gaussian Curvature in the Budding of HIV-1 Viruses. APS March Meeting 2018, abstract id.A54.004

Servuss RM et al. (1976) Measurement of the curvature-elastic modulus of egg lecithin bilayers. Biochim Biophys Acta 436(4):900–903 [PubMed: 986174]

Shi Z, Baumgart T (2014) Dynamics and instabilities of lipid bilayer membrane shapes. Adv Colloid Interface Sci 208:76–88 [PubMed: 24529968]

Simons K, Ikonen E (1997) Functional rafts in cell membranes. Nature 387(6633):569–572 [PubMed: 9177342]

Simunovic M et al. (2013) Protein-mediated transformation of lipid vesicles into tubular networks. Biophys J 105(3):711–719 [PubMed: 23931319]

Simunovic M et al. (2015) When physics takes over: BAR proteins and membrane curvature. Trends Cell Biol 25(12):780–792 [PubMed: 26519988]

Simunovic M et al. (2016) How curvature-generating proteins build scaffolds on membrane nanotubes. Proc Natl Acad Sci USA 113(40): 11226–11231. 10.1073/pnas.1606943113 [PubMed: 27655892]

Simunovic M et al. (2016a) How curvature-generating proteins build scaffolds on membrane nanotubes. Proc Natl Acad Sci USA 113(40):11226–11231 [PubMed: 27655892]

Simunovic M et al. (2016b) Physical basis of some membrane shaping mechanisms. Philos Trans Royal Soc 374(2072):20160034

Simunovic M et al. (2017) Friction mediates scission of tubular membranes scaffolded by BAR proteins. Cell 170(1):172–184. e111 [PubMed: 28648660]

Singer SJ, Nicolson GL (1972) The Fluid mosaic model of the structure of cell membranes: cell membranes are viewed as two-dimensional solutions of oriented globular proteins and lipids. Science 175(4023):720–731 [PubMed: 4333397]

Snead WT et al. (2017) Membrane fission by protein crowding. Proc Natl Acad Sci USA 114(16):E3258–E3267 [PubMed: 28373566]

Snead WT et al. (2019) BAR scaffolds drive membrane fission by crowding disordered domains. J Cell Biol 218(2):664–682 [PubMed: 30504247]

Snead WT, Stachowiak JC (2018) Structure versus stochasticity-the role of molecular crowding and intrinsic disorder in membrane fission. J Mol Biol 430(16):2293–2308 [PubMed: 29627460]

Stachowiak JC et al. (2010) Steric confinement of proteins on lipid membranes can drive curvature and tubulation. Proc Natl Acad Sci USA 107(17):7781–7786 [PubMed: 20385839]

Stachowiak JC et al. (2012a) Membrane bending by protein-protein crowding. Nat Cell Biol 14(9):944–949 [PubMed: 22902598]

Stachowiak JC et al. (2012b) Membrane bending by protein-protein crowding. Nat Cell Biol 14(9):944–949 [PubMed: 22902598]

Stachowiak JC et al. (2013) A cost-benefit analysis of the physical mechanisms of membrane curvature. Nat Cell Biol 15(9):1019–1027 [PubMed: 23999615]

Steinem C, Meinecke M (2021) ENTH domain-dependent membrane remodelling. Soft Matt 17(2):233–240

Steinkühler J et al. (2020) Controlled division of cell-sized vesicles by low densities of membrane-bound proteins. Nat Commun 11(1):1–11 [PubMed: 31911652]

Strey H et al. (1995) Measurement of erythrocyte membrane elasticity by flicker eigenmode decomposition. Biophys J 69(2):478–488 [PubMed: 8527662]

Suetsugu S et al. (2014) Dynamic shaping of cellular membranes by phospholipids and membrane-deforming proteins. Physiol Rev 94(4):1219–1248 [PubMed: 25287863]

Takamori S et al. (2006) Molecular anatomy of a trafficking organelle. Cell 127(4):831–846 [PubMed: 17110340]

Takenawa T, Itoh T (2006) Membrane targeting and remodeling through phosphoinositide-binding domains. IUBMB Life 58(5–6):296–303 [PubMed: 16754321]

Tenchov BG et al. (2013) Fusion peptides promote formation of bilayer cubic phases in lipid dispersions. An X-Ray Diffraction Study Biophys J 104(5):1029–1037 [PubMed: 23473485]

van Meer G et al. (2008) Membrane lipids: where they are and how they behave. Nat Rev Mol Cell Biol 9(2):112–124 [PubMed: 18216768]

Venable RM et al. (2015) Mechanical properties of lipid bilayers from molecular dynamics simulation. Chem Phys Lipids 192:60–74 [PubMed: 26238099]

Weise K et al. (2011) Membrane-mediated induction and sorting of K-Ras microdomain signaling platforms. J Am Chem Soc 133(4):880–887 [PubMed: 21141956]

Welman A et al. (2000) Structure and function of the C-terminal hypervariable region of K-Ras4B in plasma membrane targetting and transformation. Oncogene 19(40):4582–4591 [PubMed: 11030147]

Willumsen BM et al. (1984) The p21 ras C-terminus is required for transformation and membrane association. Nature 310(5978):583–586 [PubMed: 6087162]

Wilson JP et al. (2011) Proteomic analysis of fatty-acylated proteins in mammalian cells with chemical reporters reveals S-acylation of histone H3 variants. Mol Cell Proteomics 10(3):M110.001198

Wu H-H (2008) Historical development of the Gauss-Bonnet theorem. Sci China Ser A Math 51:777–784

Yandrapalli N et al. (2016) Self assembly of HIV-1 Gag protein on lipid membranes generates PI(4,5)P2/cholesterol nanoclusters. Sci Rep 6:39332 [PubMed: 28008947]

Zeno WF et al. (2018) Synergy between intrinsically disordered domains and structured proteins amplifies membrane curvature sensing. Nat Commun 9(1):4152 [PubMed: 30297718]

Zeno WF et al. (2019) Molecular mechanisms of membrane curvature sensing by a disordered Protein. J Am Chem Soc 141(26):10361–10371 [PubMed: 31180661]

Zhou Y et al. (2017) Lipid-sorting specificity encoded in K-Ras membrane anchor regulates signal output. Cell 168(1–2):239–251e216 [PubMed: 28041850]

Zhou Y et al. (2021a) RAS Nanoclusters selectively sort distinct lipid headgroups and acyl chains. Front Mol Biosci 8:686338 [PubMed: 34222339]

Zhou Y et al. (2021b) The KRAS and other prenylated polybasic domain membrane anchors recognize phosphatidylserine acyl chain structure. Proc Natl Acad Sci USA 118(6):e2014605118 [PubMed: 33526670]

Zhou Y, Cho K-J, Plowman SJ, and Hancock JF (2012). Nonsteroial Anti-inflammatory Drugs Alter the Spatiotemporal Organization of Ras Proteins on the Plasma Membrane, J Biol Chem, 287, 16586–16595. [PubMed: 22433858]

Zhou Y, Hancock JF (2015) Ras nanoclusters: versatile lipid-based signaling platforms. Biochim Biophys Acta Mol Cell Res 1853(4):841–849

Zimmerberg J, Kozlov MM (2006) How proteins produce cellular membrane curvature. Nat Rev Mol Cell Biol 7(1):9–19 [PubMed: 16365634]

Box 1

Contributions of Mean and Gaussian Curvatures to Membrane Bending

The plasma membrane can be regarded as a two-dimensional surface (S) that spans a three-dimensional space, which can be described by principal curvatures $k1$ and $k2$, mean curvature $J = (\frac{k1 + k2}{2})$, and Gaussian curvature $K = k1 \cdot k2$ (Helfrich 1973). The total elastic bending energy of the surface is then given by the surface integral of Eq. 1:

$$E_{\text{bending}} = \int_S d\mathbf{S}\left(\frac{1}{2}\kappa(J - c_0)^2 + \bar{\kappa}K\right),\tag{1}$$

where κ and $\bar{\kappa}$ are bending and saddle splay moduli, respectively, c_o is spontaneous curvature, and $d\mathbf{S}$ is the area element. The Gaussian curvature component of Eq. 1 can be related to surface topology and boundary line using the Gauss–Bonnet theorem (Eq. 2), which states that the integral of Gaussian curvature K over the entire surface S can be written as a contour integral of a geodesic curvature kg at the boundary line l of S, and a topological parameter called Euler characteristic X (Lee 1997).

$$\int_S K \cdot d\mathbf{S} = 2\pi X - \oint_l k_g \cdot d\mathbf{l}\,.\tag{2}$$

We refer the reader to (Wu 2008) for the history of the Gauss–Bonnet theorem. For the purposes of this review, it suffices to state that substituting the Gaussian term in Eq. 1 with the expression in Eq. 2 would allow for analyzing the topological and phase boundary components of the PM remodeling energetics. Note that cell membranes contain domains of differing phases and elasticity. Therefore, the contour integral in Eq. 2 is taken over the geodesic curvature along the domain boundary lines (Jülicher and Lipowsky 1996; Baumgart et al. 2005; Lipowsky 2022). However, for a closed membrane surface with uniform elastic properties, the term containing the contour integral vanishes, so the integral of the Gaussian curvature in Eq. 2 reduces to Eq. 3.

$$\int_S K \cdot d\mathbf{S} = 2\pi X\,.\tag{3}$$

Also note that the Euler characteristic X is invariant under a continuous bending condition. Therefore, the Gaussian component of membrane curvature contributes to the energy only when remodeling involves changes in phase boundary and/or topology.

Box 2

Small Gradient Approximation of Membrane Elastic Energy, and Coupling of Differential Areal Tension and Membrane Bending

Small gradient approximation based on Monge parameterization of differential geometry has been used to describe mean and Gaussian curvatures in terms of the height function h(x,y) above a flat reference plane, with the membrane surface represented by coordinates (x, y, h(x, y)) (Mazharimousavi, Forghani et al. 2017). The differential area S in Eq. 1 can then be written as $\sqrt{(1 + (\nabla h)^2}dxdy$. When the extent of membrane deformation is small ($\nabla h << 1$), this reduces to $1 + \frac{1}{2}(\nabla h)^2$ and the Gaussian component in Eq. 1 can be ignored. After adding a density term for the cost of area increase due to stretching of the curved surface ($\frac{1}{2}\gamma(\nabla h)^2$ where γ is surface tension), the total bending energy is expressed as the integral over the base plane (Eq. 9):

$$E_{bending} = \frac{1}{2}\int \kappa(\Delta h)^2 dxdy + \gamma(\nabla h)^2.\tag{9}$$

This implies that, under equilibrium conditions, areal strain and curvature stress are coupled, so that the strain caused by the insertion of a SBMP into a monolayer is balanced by curvature. We refer the reader to the work of Markus Deserno (2015) for in depth analysis of this issue.
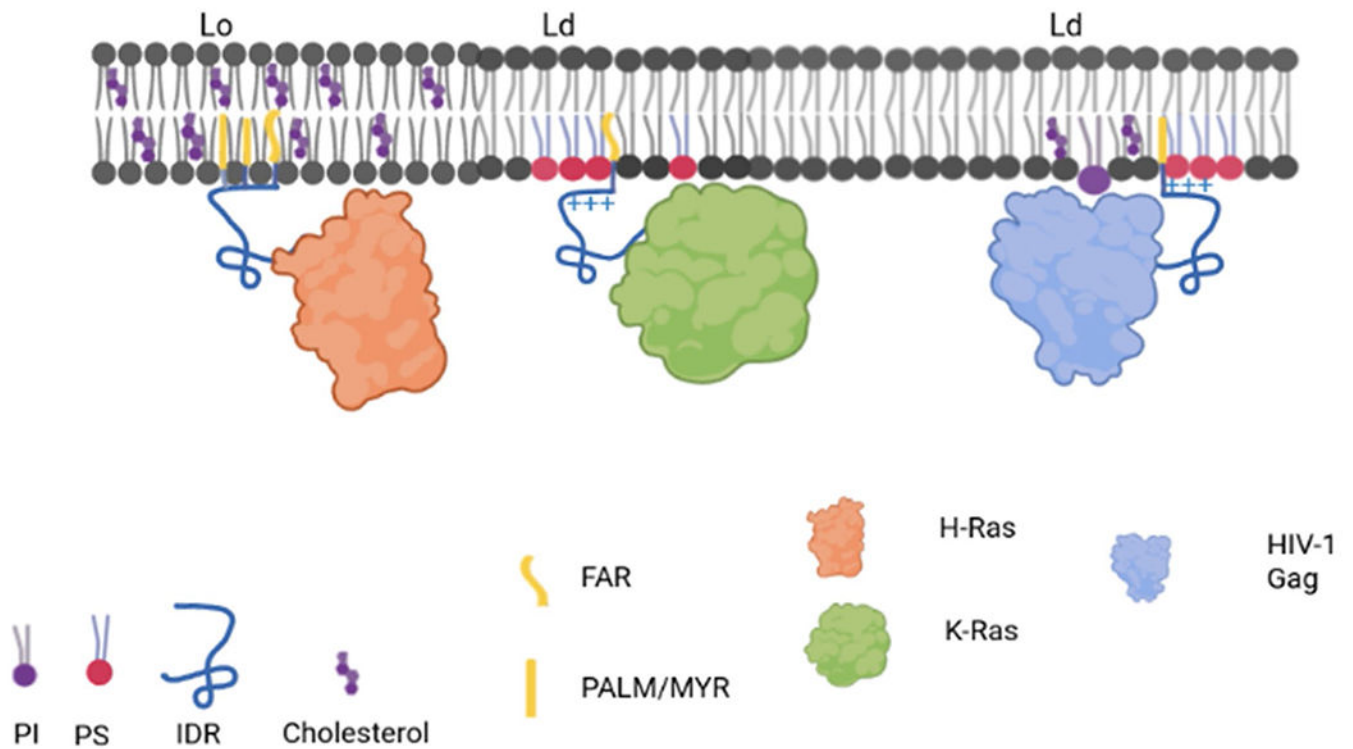
Fig. 1.
HRas, KRas and HIV Gag as examples of PM remodeling by binding of SBMPs with lipidated IDRs. Highlighted here is membrane remodeling by the insertion of a lipid motif and charge interactions between polybasic residues of IDRs and head groups of anionic phospholipids. The charge interaction leads to the clustering of anionic phospholipids around the protein. Farnesylation (Far), palmitoylation (Palm) and myristoylation (Myr) of IDRs are utilized for selective PM anchoring and remodeling in liquid-ordered (Lo) and liquid-disordered (Ld) domains
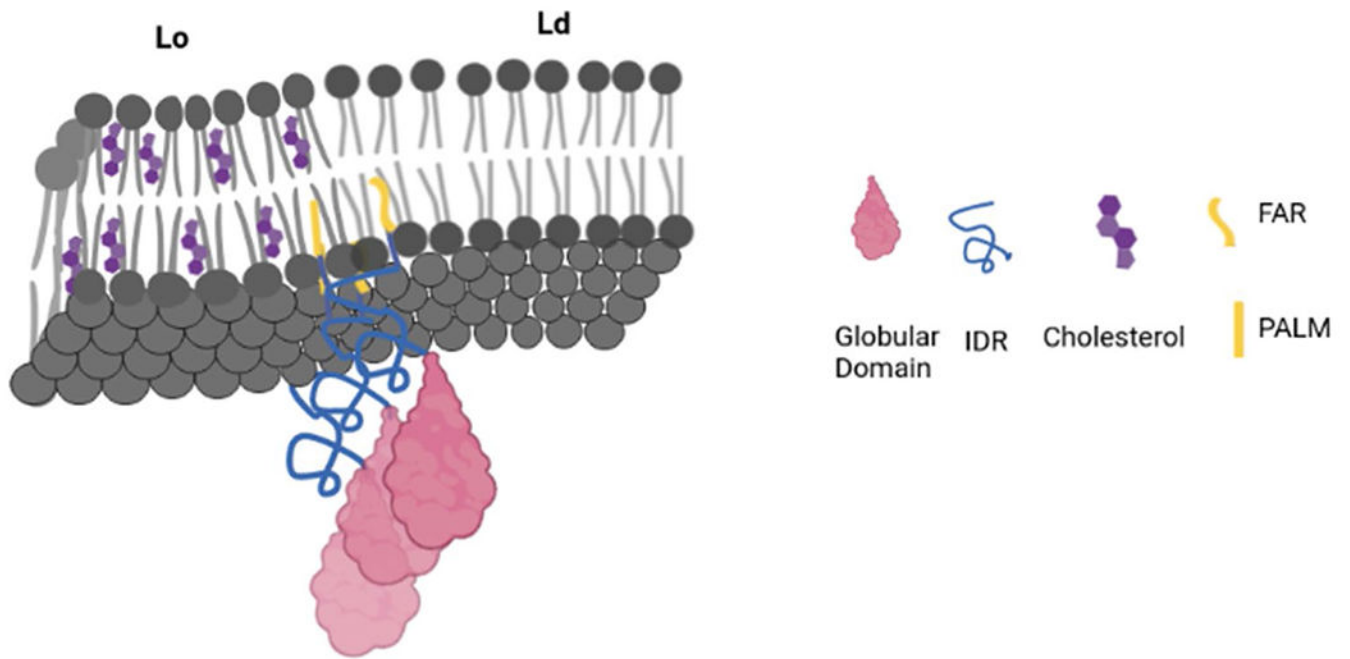
Fig. 2.
A scenario of PM remodeling by SBMP aggregates with lipidated IDRs. The schematic
shows the deformation of a two-domain (Lo/Ld) membrane by the asymmetric insertion and
clustering of lipid-modified proteins, highlighting a specific instance in which the aggregate
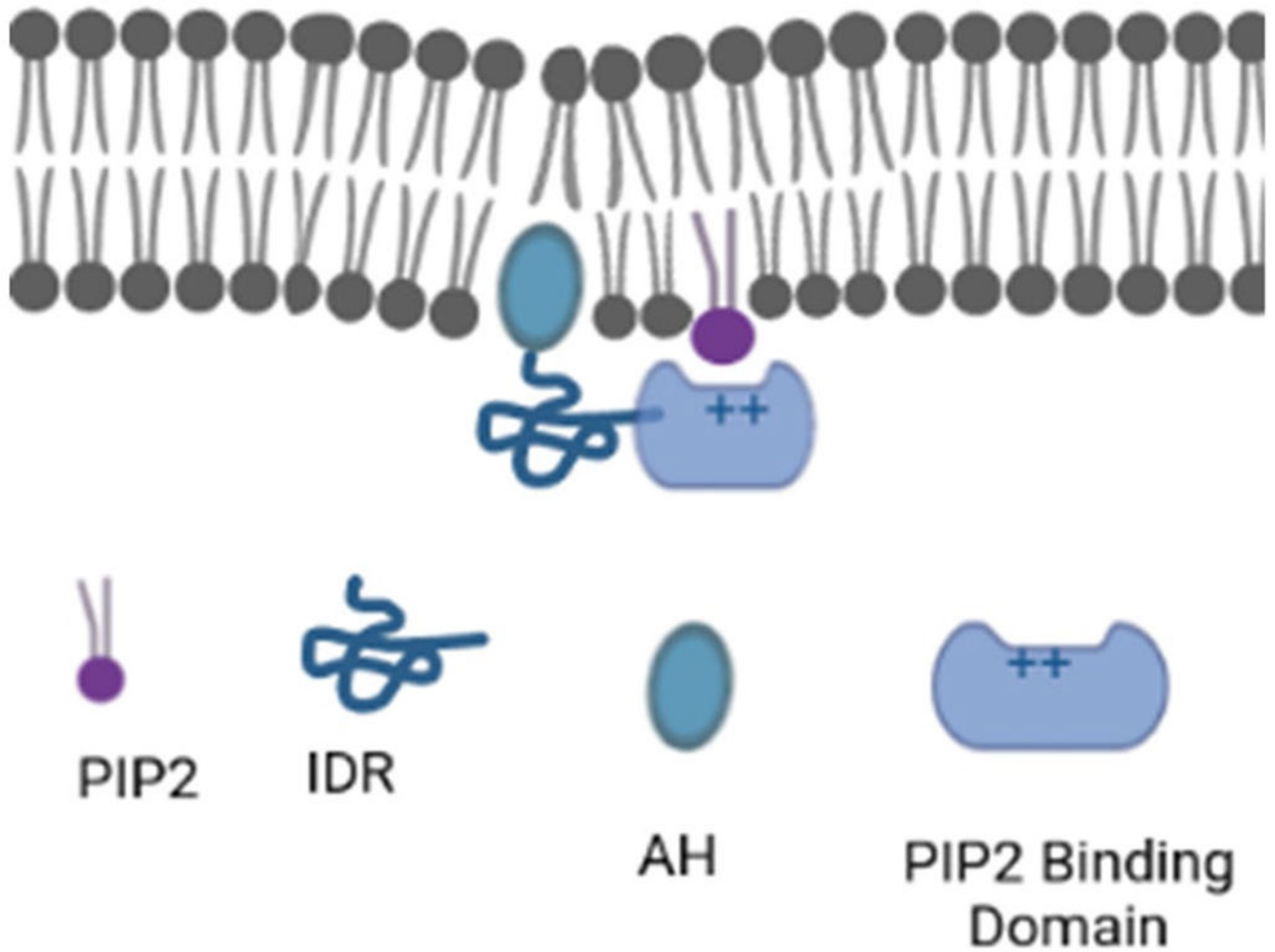stabilizes the domain interface as the pivot/center of deformation

Fig. 3.
PM remodeling by binding of SBMPs with non-lipidated IDRs. Membrane anchoring and deformation with the insertion/wedging of an amphipathic helix (AH) and recognition of anionic phospholipid head groups (PIP_2 in this case) by the protein structure/motif within the globular domain is shown. Insertion of an AH increases the area of one of the leaflets (lower leaflet in the schematic), and a positive membrane curvature is induced to compensate for this increase in surface area
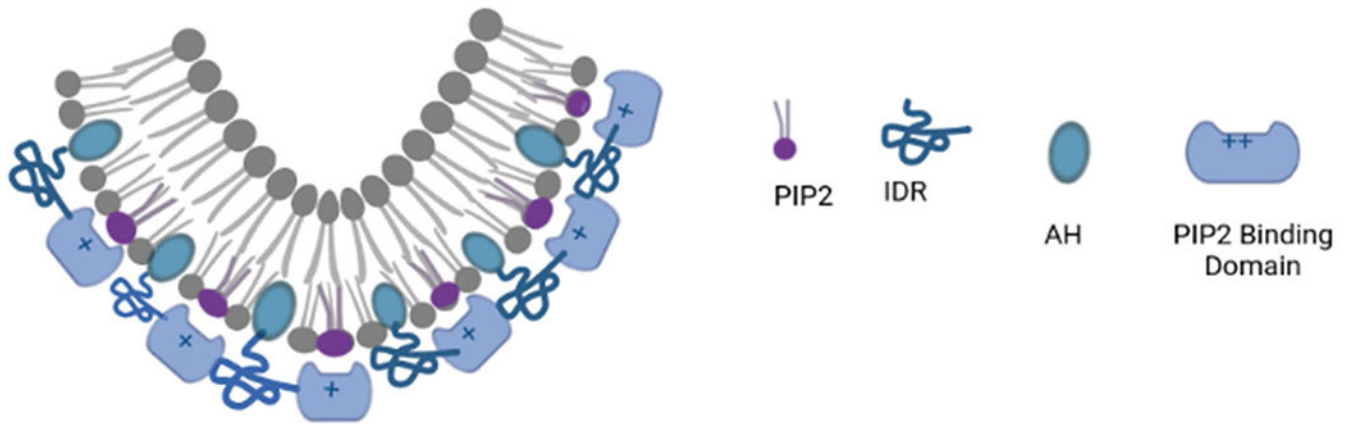
Fig. 4.
PM remodeling by SBMP aggregates with non-lipidated IDRs. This includes Induced-bending via the combined effects of AH insertion and the generation of lateral pressure from the asymmetric aggregation of non-lipidated SBMP. The IDR may sample various degree of compactness, with the radius of gyration of the IDR as well the concentration of the bound protein contributing to membrane bending in addition to the size of the AH and the subsequent increase in monolayer surface area